Journal Name

ARTICLE

Formation of lipid membrane-incorporated small π-molecules bearing hydrophilic groups

Atsushi Ikeda,* Kengo Ashizawa, Yuki Tsuchiya, Masafumi Ueda and Kouta Sugikawa

Received 00th January 20xx,
Accepted 00th January 20xx

DOI: 10.1039/x0xx00000x

www.rsc.org/

Nineteen poorly water-soluble π-conjugated molecules were evaluated in terms of their ability to be stably incorporated into lipid membranes. The resulting lipid membrane-incorporated π-conjugated guest molecules (LMIGs) were classified into four categories, including (i) those that formed stable LMIGs; (ii) those where some of guest molecules precipitated; (iii) those that formed small self-aggregates consisting of lipids and/or guest molecules; and (iv) those that leaked some of the guest molecules into the bulk water. Compounds belonging to category (ii) were confirmed by UV-vis absorption analysis. In contrast, compounds belonging to categories (i), (iii) and (iv) were discriminated based on their ^{1}H NMR spectra and the broadening or disappearance of the peaks of the guest molecules and the lipids in LMIGs and large liposomes. Several LMIGs could be converted from one category to another using other lipids. Furthermore, the guest molecules belonging to category (iv) were successfully predicted using the octanol-water partition coefficient, which was calculated by simulation.

1. Introduction

Liposomes have recently attracted considerable interest as suitable materials for the development of drug-delivery systems (DDSs), where therapeutic agents can be encapsulated by a vesicle or polymeric material (e.g., DNA) can be adsorbed on the outside of a vesicle.[1–9] The advantages of liposomes include their lower cost, ease of large-scale manufacture and ability to evade immune and inflammatory responses.[10] However, it is not yet known whether poorly water-soluble π-conjugated drug molecules can be incorporated into lipid membranes. There are two main factors involved in determining the stability (or formation) of lipid membrane-incorporated π-conjugated guest molecules (LMIGs), including (i) the affinity of the guest molecule for the alkyl chains of the lipids; and (ii) the self-aggregation of the guest molecules in the lipid membranes. Factor (ii) can affect the long-term stability of LMIG solutions, which can be improved by inhibiting the self-aggregation of the guest molecules.[11,12] In contrast, factor (i) determines whether all of the guest molecules can form LMIGs. In the case of there being low affinity between the guest molecules and the alkyl chains of the lipids, the hydrophobic guest molecules can precipitate from solution outside of the lipid membranes by conventional methods. However, we recently succeeded in preparing LMIGs from several hydrophobic guest molecules without the formation of any precipitates from the prerequisite cyclodextrin complexes using the exchange method in lipid membranes.[11–26] However, the use of guest compounds bearing

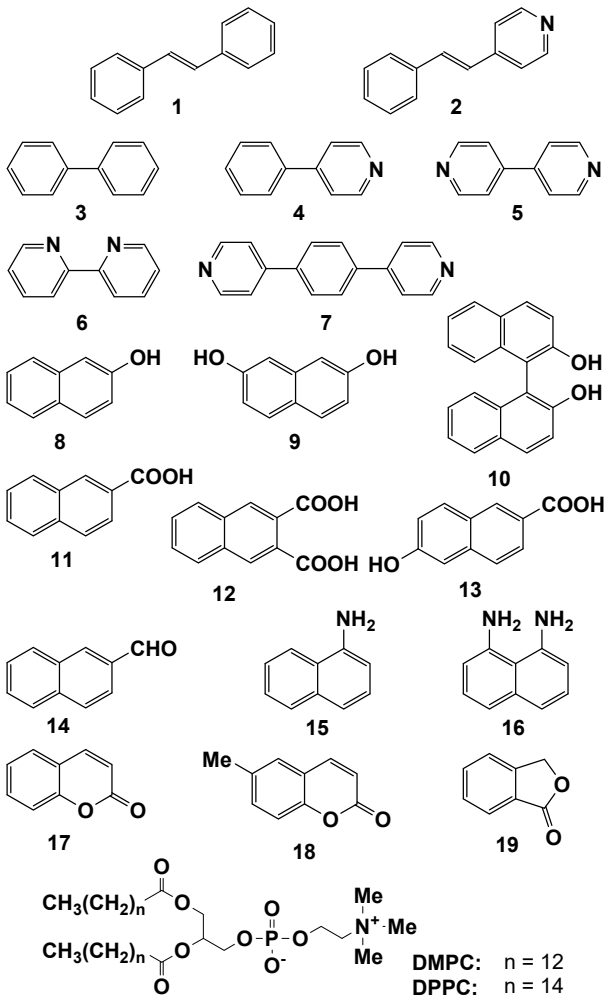

Department of Applied Chemistry, Graduate School of Engineering, Hiroshima University, 1-4-1 Kagamiyama, Higashi-Hiroshima 739-8527, Japan. E-mail: aikeda@hiroshima-u.ac.jp

†Electronic Supplementary Information (ESI) available: UV-vis absorption and ^{1}H NMR spectra. See DOI: 10.1039/x0xx00000x

a hydrophilic moiety could result in some leakage from the lipid membranes. This type of leakage is a very important factor for the preparation of LMIGs based on guest molecules or drugs and liposomes. Schwarzenbach *et al*. recently reported a method for determining the liposome-water distribution ratios (log K_{lipw}) of substituted phenols and several other compounds.[27–31] Although this value can be useful for evaluating the affinity of a guest molecule for lipid and cell membranes, it still remains difficult to determine whether guest molecules have been successfully incorporated into liposomes at high concentrations. In this paper, we have ^{1}H NMR spectroscopy to determine the leakage percentages of guest molecules from liposomes. The results of this study have shown that LMIGs were not only labilized by the guest molecules towards leaking their guest molecules into water but that they also formed small self-aggregates with lipids. Furthermore, we have investigated the relationship between the equilibrium and the octanol-water partition coefficient (log P_{ow}) for some model small π-compounds (**1**–**19**) and confirmed the threshold values log P_{ow} for these systems.[28]

2. Experimental

2.1. Experimental materials

trans-Stilbene (**1**), 4-styrylpyridine (**2**), 4-phenylpyridine (**4**), 4,4'-bipyridyl (**5**), 2,2'-bipyridyl (**6**) and 2,3-naphthalenedicarboxylic acid (**12**) were purchased from Wako Pure Chemical Industries Ltd (Tokyo, Japan). Biphenyl (**3**), 1,4-di(4-pyridyl)benzene (**7**), 2-naphthol (**8**), naphthalene-2,7-diol (**9**), 1,1'-bi-2-naphthol (**10**), 2-naphthoic acid (**11**), 6-hydroxy-2-naphthoic acid (**13**), 2-naphthalenecarbaldehyde (**14**), naphthalene-1-amine (**15**), naphthalene-1,8-diamino (**16**), coumarin (**17**), 6-methylcoumarin (**18**) and phthalide (**19**) were purchased from Tokyo Chemical Industries Co., Ltd. (Tokyo, Japan). 1,2-Dimyristoyl-*sn*-glycero-3-phosphocholine (DMPC) and 1,2-dipalmitoyl-*sn*-glycero-3-phosphocholine (DPPC) were obtained from NOF Corp. (Tokyo, Japan) and Avanti Polar Lipids, Inc. (Alabaster, AL, USA), respectively

2.2. Preparation of lipid membrane-incorporated guest molecules (LMIGs)

Solutions of DMPC or DPPC (4.00×10^{-6} mol) and compounds **1**–**19** in chloroform (0.1 mL) were concentrated on a rotary evaporator at 40 °C. The compositions of the mixtures were as follows: [**1**–**19**]/[DMPC] = 5.0, 10.0 and 20.0 mol%. Pure water (1.0 mL) was added and the aqueous mixture was agitated on a vortex mixer for 1 min. To resulting multilamellar vesicles were subjected to eight freeze-thaw cycles and extruded eleven times (LiposoFast-Basic; Avestin Inc., Ottawa, Canada) through two stacked polycarbonate membranes (pore size 50 nm) to afford unilamellar vesicles. The final lipid concentration was 4.0 mM.

2.3. Cryogenic-Temperature Transmission Electron Microscopy (Cryo-TEM)

Cryo-TEM samples were prepared using a universal cryofixation and cryopreparation system (Leica EM CPC, Wetzlar, Germany). The isolated chamber was humidified to near saturation prior to the introduction of the sample to avoid the evaporation of water from the sample. Sample droplets (2–3 mL) were placed on a microperforated cryo-TEM grid and absorbed on to a filter paper. This process resulted in the formation of thin liquid films of 10–300 nm in thickness that freely spanned the micropores of a carbon-coated lacelike polymer layer supported by a metal mesh grid. After a minimum hold time of 30 s, the sample grid assembly was rapidly vitrified with liquid ethane at its melting temperature (–163 to –170 °C). A hold time was adopted to relax any deformations in the flow that may have occurred during the blotting process. The vitreous specimen was kept under liquid nitrogen prior to being loaded into a cryogenic sample holder (Gatan 626-DH). Imaging was performed on a JEOL JEM-3100 FEF instrument operating at 300 kV (Tokyo, Japan). The use of a minimal dose system (MDS) was necessitated by the electron radiation sensitivity of the sample being probed. Images were recorded on a Gatan 794 multiscan digital camera (Gatan Inc., Pleasanton, CA, USA) and processed using version 3.8.1 of the DigitalMicrograph software (Gatan Inc., Pleasanton, CA, USA). The optical density gradients of the background, which are normally ramp-shaped, were digitally corrected using a custom-made subroutine that is compatible with DigitalMicrograph.

3. Results and discussion

3.1. Formation of LMIGs by the premixing method

Lipid membrane-incorporated compounds **1**–**19** (LMI**1**–**19**) consisting of dimyristoylphosphatidylcholine (DMPC) were prepared according to a previously reported premixing method (Scheme S1).[10,32] Briefly, the LMIGs were prepared by dissolving the lipids and the guest molecules in a suitable organic solvent, followed by concentration of the resulting mixture to give a residue, which was extracted with water. Most of the benzene derivatives were evaporated during the concentration step together with the organic solvents. For this reason, we used naphthalene, biphenyl and coumarin derivatives or their analogues as guest molecules. LMI**1** has been reported previously.[33,34]

3.2 Aqueous solubilization of guest molecules

3.2.1 The effect of adding pyridyl groups. 4-Styrylpyridine (**2**), 4-phenylpyridine (**4**), 4,4'-bipyridine (**5**), 2,2'-bipyridine (**6**) and 1,4-di(4-pyridyl)benzene (**7**) were used as guest molecules to investigate the impact of adding a hydrophilic pyridyl moiety. The solubilities of compounds **2** and **4**–**7** in the liposomes were determined by measuring the absorbance values of [**2**, **4**–**7**]/[DMPC] at 308, 256, 240, 281 and 282 nm, respectively, after subtracting the scattering of the DMPC liposomes (Figs. 1 and S1). The dashed lines shown in Fig. 1 represent the extrapolated absorbance values corresponding to the dissolution of 100% of the guests in water. The absorbance values of LMI**2**, **4**–**6** lay on the extrapolated lines below 10 mol%. It is noteworthy that

similar results have been observed for stilbene (**1**) and biphenyl (**3**), neither of which contains a pyridyl moiety. These results therefore suggest that the inclusion of a pyridyl moiety scarcely affected the formation of the LMIGs. In contrast, the absorbance of LMI**7** was saturated above 5 mol% (Fig. 1 green circle), indicating that the maximum tolerated ratio of **7** was less than 5 mol%, making it lower than those of the other pyridyl derivatives prepared by the premixing method.

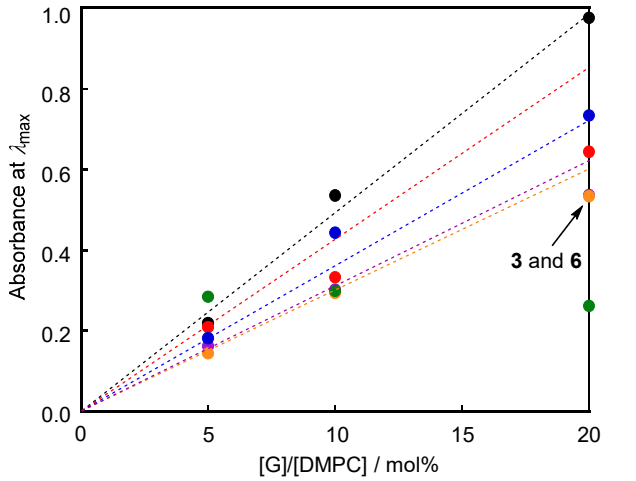

Fig. 1 UV-vis absorption spectra of the LMIGs ([**2**–**7**]/[DMPC] = 2.5, 5.0 and 20.0 mol%, [**2**–**7**] = 0.2 mM). The absorbance (Abs) at λ_{max} versus [G]/[DMPC] in the LMIGs. The λ_{max} values were 308, 253, 256, 240, 281 and 282 nm for LMI**2** (black circle), LMI**3** (purple circle), LMI**4** (red circle), LMI**5** (blue circle), LMI**6** (orange circle) and LMI**7** (green circle), respectively. All of these absorption spectra were obtained by subtracting the light scattering of the DMPC liposomes and were measured in water at 25 °C (1 mm cell).

3.2.2. The effect of adding a hydrophilic group to the naphthalene derivatives. Compounds **8**–**16** are naphthalene derivatives containing a variety of different hydrophilic groups. The absorbance values of LMI**8** and LMI**9** bearing hydroxy groups were consistent with the extrapolated lines for concentrations of less than 10 mol%, but deviated from the lines at a concentration of 20 mol%. A similar trend was also observed for LMI**14** bearing a formyl group (Fig. 2 black, purple and green circles). The absorbance peaks of 20 mol% solutions of LMI**8**, LMI**9** and LMI**14** did not show any peak broadening (Fig. S2A, S2B and S2F). Furthermore, no precipitation was observed in these samples. This deviation was therefore attributed to compounds **8**, **9** and **14** not being incorporated into the liposomes at 20 mol%, with the compounds being removed by filtration through the membranes (pore size 50 nm) during the extrusion process. In contrast, the absorbance values of LMI**10** bearing two naphthol units; LMI**11** and LMI**13** bearing carboxy groups; and LMI**15** and LMI**16** bearing amino groups were consistent with the extrapolated lines up to a concentration of 20 mol% (Figs. 2, S2C–E, S3A and S3B). These results indicated that these guest molecules were well dispersed in water in the presence of liposomes up until a concentration of 20 mol%. Although several attempts were made to solubilize compound **12** bearing two carboxy groups in several organic solvents, the concentrations of **12** were too low to allow for the preparation of LMI**12** using the premixing method.

3.2.3. The effects of lactone derivatives. To evaluate the effect of adding a lactone moiety, we examined the water-solubilization properties of coumarin (**17**), 7-methylcoumarine (**18**) and phthalide (**19**). The solubilities of compounds **17**–**19** were determined based on the absorbance of [**17**–**19**]/[DMPC] at 320 nm using the procedure described above for compounds **1**–**16**. The absorbance values of LMI**17**–**19** were all consistent with the extrapolated lines for concentrations below 10 mol%, suggesting that most of the molecules of **17**–**19** had successfully dissolved in the water (Figs. 3 and S3C–E).

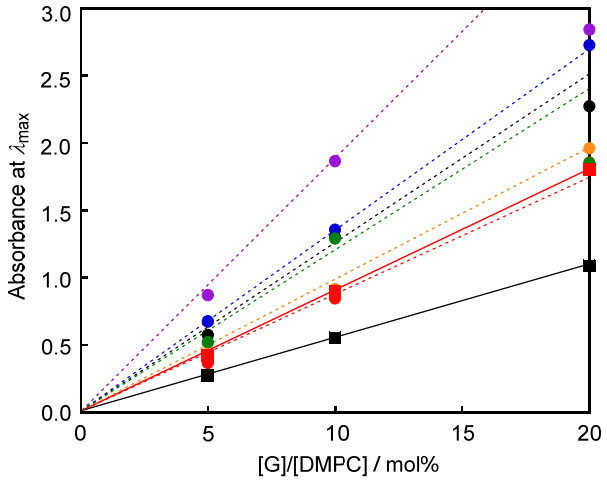

Fig. 2 UV-vis absorption spectra of the LMIGs ([**8**–**11** or **13**–**16**]/[DMPC] = 2.5, 5.0 and 20.0 mol%, [**8**–**11** or **13**–**16**] = 0.2 mM). The absorbance (Abs) at λ_{max} versus [G]/[DMPC] in the LMIGs. The λ_{max} values were determined to be 229, 235, 231, 250, 287, 242 and 223 nm for LMI**8** (black circle and dashed line), LMI**9** (purple circle and dashed line), LMI**10** (red circle and dashed line), LMI**11** (blue circle and dashed line), LMI**13** (orange circle and dashed line), LMI**14** (green circle and dashed line), LMI**15** (black square and solid line) and LMI**16** (red square and solid line), respectively. All of the absorption spectra were obtained by subtracting the light scattering from the DMPC liposomes and were measured in H_2O at 25 °C (1 mm cell). [DMPC] = 4.0 mM for **8**, **9**, **11** and **13**–**16**, [DMPC] = 2.0 mM for **10**.

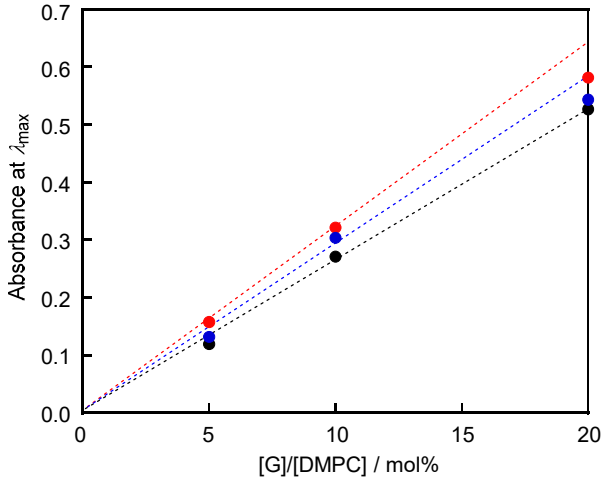

Fig. 3 UV-vis absorption spectra of the LMIGs ([**17**–**19**]/[DMPC] = 2.5, 5.0 and 20.0 mol%, [**17**–**19**] = 0.2 mM). The absorbance (Abs) at λ_{max} versus [G]/[DMPC] in the LMIGs. The λ_{max} values were determined to be 278, 278, 231 and 239 nm for LMI**17** (black circle), LMI**18** (red circle) and LMI**19** (blue circle), respectively. All of the absorption spectra were obtained by subtracting the light scattering from the DMPC liposomes and were measured in H_2O at 25 °C (1 mm cell). [DMPC] = 4.0 mM.

3.3 Determination of formation of LMIGs by ^{1}H NMR analyses

3.3.1 Formation of lipid membrane-incorporated aromatic compounds bearing pyridyl groups. Compounds **1**–**6** dissolved in water in the presence of the DMPC liposomes at a concentration of [**1**–**6**]/[DMPC] = 10 mol%, making it possible to confirm the formation of the LMIGs by ^{1}H NMR analysis at 10 mol% (Figs. 4B–4G and S4). The ^{1}H NMR spectra of the LMIGs did not contain any peaks that could be assigned to DMPC or the guest molecules in the LMIGs because of the extreme broadening of the signals following the formation of the liposomes (Fig. 4A). The appearance of any peaks assignable to DMPC or the guest molecules would therefore indicate that the DMPC and guest molecules had been released from the liposomes. The peak intensities in Figs. 4A–4G and S4 were normalized relative to the value of DMSO (0.4 mM), which was adopted as an internal standard. As shown in Fig. 4B, no signals were observed for DMPC or **1**, indicating that all of the molecules of DMPC and **1** had formed LMI**1** (Scheme 1A). Similar results were observed for compounds **2** and **3** (Fig. 4C and 4D). Fig. 4E–4G shows that the addition of compounds **4**–**6** to a solution of DMPC liposomes did not lead to the appearance of any new peaks in the range of 0.8–1.4 ppm, which were attributed to the alkyl chains of free DMPC, but did result in the appearance of several new peaks assignable to **4**–**6**. These results clearly indicated that several molecules of **4**–**6** had leaked from the lipid membranes into the bulk aqueous environment, where they had dissolved without the assistance of DMPC (Scheme 1D). The leakage percentages of **4**–**6** were determined to be 5, 59 and 36%, respectively, based on the peak intensities of compounds **4**–**6** relative to the DMSO peak.

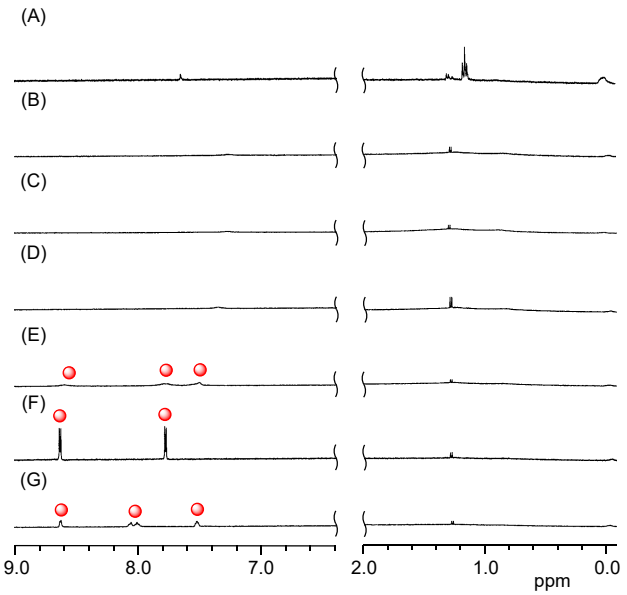

Fig. 4 Partial ^{1}H NMR spectra of (A) the DMPC liposome, (B) LMI**1**, (C) LMI**2**, (D) LMI**3**, (E) LMI**4**, (F) LMI**5** and (G) LMI**6** in D_2O at 25 °C (●: free guest molecule). [**1**–**6**]/[DMPC] = 10.0 mol%, [DMPC] = 4.0 mM, [DMSO] = 0.4 mM.

3.3.2. Formation of lipid membrane-incorporated naphthalene derivatives. With the exception of **12**, compounds **8**–**16** dissolved in D_2O containing DMPC at a concentration of less than 10 mol%, allowing their ^{1}H NMR spectra to be measured at 10 mol%. As shown in Figs. 5C, 5D, 5H, S5 and S6, several new broad peaks were observed in the ^{1}H NMR spectra of LMI**10**, **11** and **16** bearing hydroxy, carboxy or amino groups in the range of 0.8–1.4 ppm, which were attributed to the alkyl chains of DMPC. If the DMPC liposomes remained as large hollow particles with a diameter greater than 70 nm, then these broad peaks would not be observed because of the extreme broadening of the signals. These results therefore suggested that some of the DMPC liposomes had collapsed, with some of DMPC lipids forming small aggregates such as micelles or very small liposomes with **10**, **11** or **16** (Scheme 1C). Given that the peak intensities of DMPC are greatly dependent on the size of its aggregates, it is not possible to determine the concentration DMPC in a small aggregate based on the peak intensities in the range of 0.8–1.4 ppm. However, because larger peaks were observed in the range of 0.8–1.4 ppm for LMI**10**, compound **10** was adjudged to have destabilized the DMPC liposomes to a much greater extent than compounds **11** and **16**. In contrast, the ^{1}H NMR spectra of compounds **8**, **9** and **13**–**15** contained no peaks assignable to DMPC in the range of 0.8–1.4 ppm, despite being similar in structure to compound **11** (Fig. 5A, 5B, 5E, 5F and 5G). Furthermore, no peaks assignable to **8**, **9** and **13**–**15** were observed by ^{1}H NMR analysis in the range of 7.0–9.0 ppm, which suggested that the vast majority of these compounds had been successfully incorporated into the lipid membranes. This result therefore indicated that LMI**8**, LMI**9** and LMI**13**–**15** were stable once they had formed (Scheme 1A).

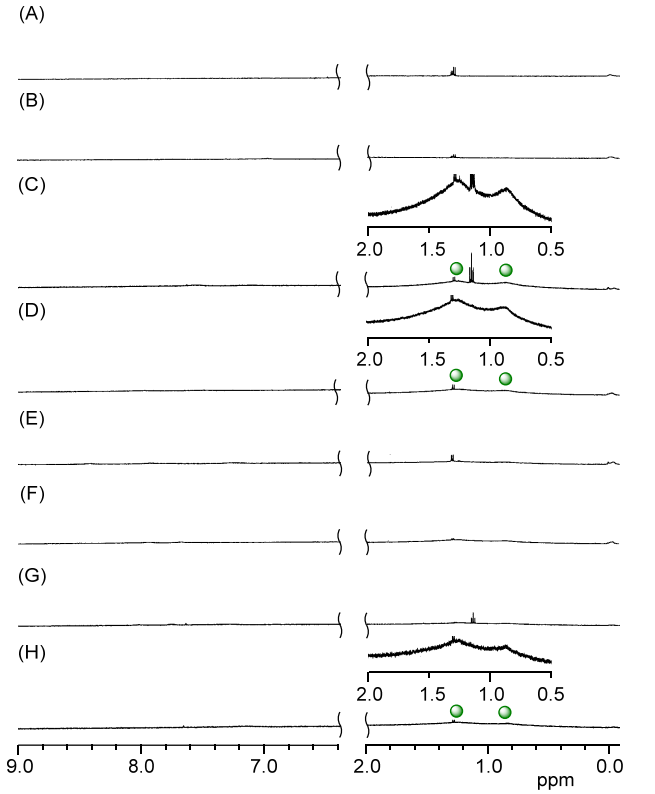

Fig. 5 Partial ^{1}H NMR spectra of (A) LMI**8**, (B) LMI**9**, (C) LMI**10**, (D) LMI**11**, (E) LMI**13**, (F) LMI**14**, (G) LMI**15** and (H) LMI**16** in D_2O at 25 °C (●: DMPC lipid). [**8**–**11** or **13**–**16**]/[DMPC]

= 10.0 mol%, [DMPC] = 4.0 mM, [DMSO] = 0.4 mM. The insets show the region of 0.5–2.0 ppm.

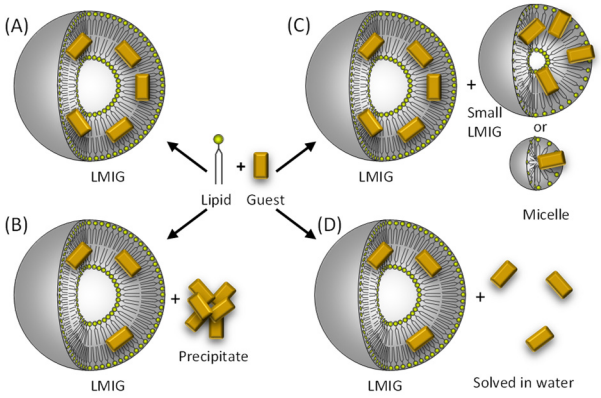

Scheme 1 Schematic illustration of (A) stable LMIG [category (i)], (B) the precipitation of the guest molecules released from LMIG [category (ii)], (C) the formation of small aggregates between the guest molecules released from LMIG and the lipids [category (iii)] and (D) the dissolution of the guest molecules released from LMIG in water [category (iv)].

3.3.3. Formation of lipid membrane-incorporated lactone derivatives. As shown in Figs. 6A–6C and S7, the ^{1}H NMR spectra of LMI**17**–**19** contained several new peaks in the range of 6.4–8.2 ppm, which were assignable to compounds **17**–**19**. In contrast, no new peaks were observed in the range of 0.8–1.4 ppm for compounds **17**–**19**. These results suggested that the DMPC liposomes did not collapse in the presence of these guest compounds and that several molecules of **17**–**19** had leaked from the lipid membranes to the bulk water, where they dissolved without any assistance from DMPC. The leakage percentages of **17**–**19** were determined to be 49, 40 and 100%, respectively, based on the peak intensities of compounds **17**–**19** relative to DMSO (Table 1). The leakage percentage of **18** (40%) was lower than that of **17** (49%), most likely because of the hydrophobicity of the methyl group in **18**. In contrast, the leakage percentage of **19** (100%) was much higher than those of **17** and **18**. The reason for this difference will be discussed in detail below in the section 3.4.3.

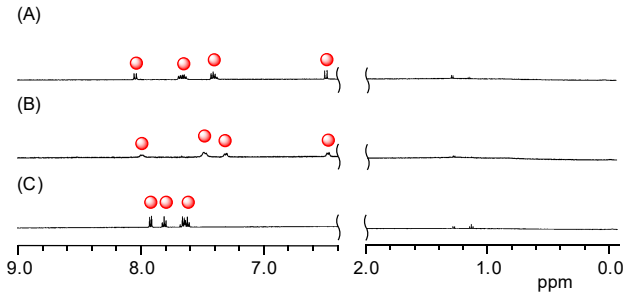

Fig. 6 Partial ^{1}H NMR spectra of (A) LMI**17**, (B) LMI**18** and (C) LMI**19** in D_2O at 25 °C (●: free guest molecule). [**17**–**19**]/[DMPC] = 10.0 mol%, [DMPC] = 4.0 mM, [DMSO] = 0.4 mM.

3.4 Abundance of the guest molecules in lipid membranes

These phenomena can be classified into four different categories when [G]/[lipid] = 10 mol%, including (i) most of the guest molecules form stable LMIGs (Scheme 1A); (ii) some of the guest molecules precipitate from solution (Scheme 1B); (iii) some of the guest molecules form small aggregates such as micelles or very small liposomes with the lipids (Scheme 1C); and (iv) some of the guest molecules are released from the lipid membranes (Scheme 1D). For category (i), the guest molecules would have a high affinity for the acyl chains of the lipids. In contrast, the guest molecules in category (ii) would have a lower affinity for the acyl chains of the lipids than those in category (i). The fullerenes and porphyrins prepared in the current study using the premixing method would therefore belong in category (ii).[11,23] However, given that LMIfullerenes and LMIporphyrins can also be prepared using an exchange method with cyclodextrins,[11–26] the guest molecules in category (ii) would be incorporated into the lipid membranes if they were included in cyclodextrins. Categories (iii) and (iv) will be discussed in detail in the following sections.

Table 1 Log P_{OW} and leakage percentage values for compounds **1–19**

Compound	log P_{OW}[a]	Leakage percentage[b]		Category
		DMPC liposome	DPPC liposome	
1	4.83	0		(i)
2	3.34	0		(i)
3	3.98	0		(i)
4	2.59	5	0	(iv) and (i)
5	1.20	59	72	(iv) and (iv)
6	1.28	36	15	(iv) and (iv)
7	2.86	–[c]		(ii)
8	2.71	0		(i)
9	1.98	0		(i)
10	4.44	0	0	(iii) and (i)
11	3.13	0	2	(iii) and (iv)
12	2.04	–[d]		(ii)
13	2.39	0		(i)
14	2.87	0		(i)
15	2.17	0		(i)
16	0.88	0	2	(iii) and (iv)
17	1.39	49	46	(iv) and (iv)
18	1.85	40	37	(iv) and (iv)
19	0.99	100	29	(iv) and (iv)

[a]Log P_{ow} was calculated using version 11.02 of the Advanced Chemistry Development Software (ACD/labs., Toronto, Canada). [b]The leakage values were determined by ^{1}H NMR spectroscopy. [c]Some of the guest molecules precipitated out for [G]/[DMPC] = 10 mol%. [d]The guest molecules did not dissolve in any organic solvents.

3.4.1 Formation of small aggregates. Compounds **10, 11** and **16** were included in category (iii) (Table 1). Although the guest molecules in category (iii) labilized the LMIGs in the same way as those belonging to categories (ii) and (iv), the guest molecules in the labilized LMIGs were not solely released from the liposomes but were also included in the small aggregate released by the fission of the liposomes. We initially considered that the dipole moments of the guest molecules could play an important role in determining whether they formed aggregates. However, this hypothesis was discarded when we established that **14** (3.0 D) formed no aggregate despite having larger dipole moment than **11** (2.5 D). Although the underlying mechanism of this process currently remains unclear, there are similarities

between these phenomena and the formation of micelles following the surfactant-mediated collapse of liposomes under aqueous conditions.[35,36] Furthermore, it has been reported that the incorporation of some guest molecules can lead to a decrease in the diameter of the liposome.[37,38] Such decreases in the diameter can be caused by local increases in the curvature of the liposome, which occur as a geometric consequence of the incorporation of a cone-like guest molecules into a phospholipid bilayer. We analyzed the LMIGs in category (iii) by dynamic light scattering (DLS) and cryogenic transmission electron microscopy (cryo-TEM) analyses to determine whether the small aggregates formed in these cases were micelles or very small liposomes. The results of the DLS measurements revealed that the hydrodynamic diameters (D_{hy}) and polydispersity indices of the liposomes barely changed for [G]/[lipid] = 10 mol% (Table 2). This result suggested that while some of the liposomes had collapsed to form small aggregates most of them remained unchanged. This idea was also supported by the following two experimental results. Although we were unable to accurately calculate the peak intensities of DMPC because of considerable peak broadening, the percentages of DMPC in the small aggregates were estimated to be approximately 25, 7 and 8% for **10**, **11** and **16**, respectively. These results showed that less than 25% of the liposome had broken down to form small aggregates. The cryo-TEM images revealed that fewer liposomes were observed in the presence of **10** ([**10**]/[DMPC] = 10 mol%) than there were in the absence of **10** (Fig. 7). Furthermore, the size of the liposomes remained almost constant regardless of the presence or absence of **10** (Fig. 7). We supposed that the aggregates were too small to be observed by cryo-TEM.

Table 2 Hydrodynamic diameters (D_{hy}) of the DMPC liposome, as determined by dynamic light-scattering at 25°C in the absence and the presence of the guest molecules or surfactant.

Guest molecule	[G]/[DMPC] / mol%	Hydrodynamic diameter / nm	Polydispersity index
–	0	88	0.12
10	10	83	0.11
10	30	101	0.16
11	10	79	0.18
16	10	91	0.10
TX-100	10	135	0.30
TX-100	30	74	0.32
TX-100	1000	8	0.27

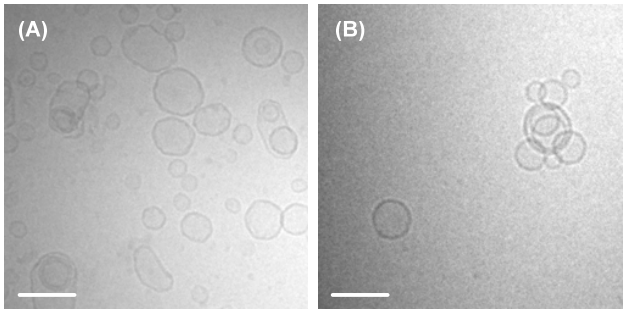

Fig. 7 Cryo TEM images of (A) DMPC liposome and (B) LMI**10**. [**10**]/[DMPC] = 30.0 mol%, [DMPC] = 1.0 mM.

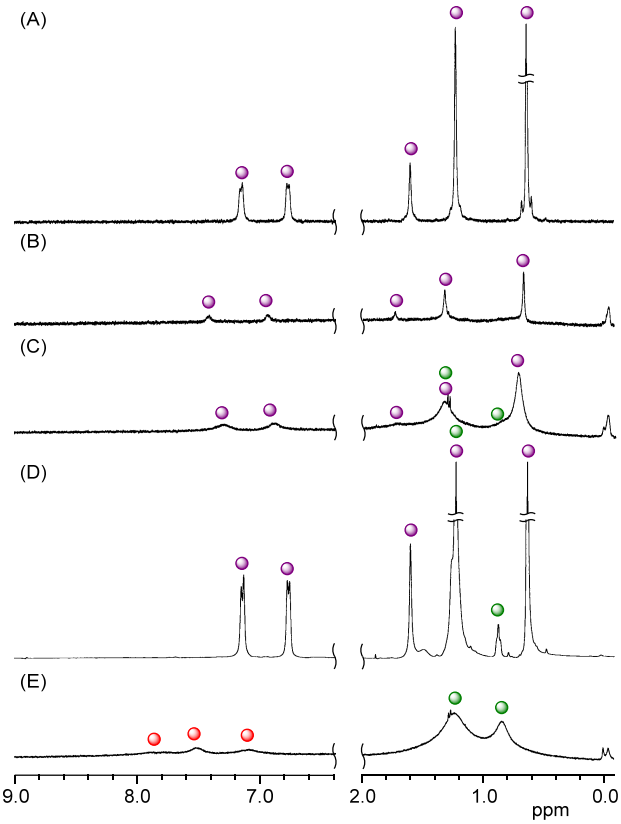

Fig. 8 Partial ^{1}H NMR spectra of (A) TX-100, DMPC-TX-100 mixtures with [TX-100]/[DMPC] = (B) 10.0, (C)30.0 and (D) 1000 mol% and (E) LMI**10** with [**10**]/[DMPC] = 30.0 mol% in D_2O at 25 °C (●: guest molecule, ●: TX-100 and ●: DMPC lipid in the small aggregates). [DMPC] = 1.0 mM, [DMSO] = 0.1 mM.

It is well known that liposomes can collapse and form micelles after the addition of a large amount of a suitable lysing agent (*e.g.*, ethanol) or a surfactant under aqueous conditions.[39,40] If the model described in category (iii) is correct, we would expect compounds **10**, **11** and **16** to act as surfactants. With this in mind, we compared the effects of adding the nonionic surfactant triton-X 100 (TX-100) to LMI**10**. For [TX-100]/[DMPC] = 10 mol%, ^{1}H NMR analysis revealed the slightly broadened peaks of TX-100, as shown in Figs. 8B and S8B (purple circles). When the concentration was increased to 30 mol%, ^{1}H NMR analysis showed that there was a considerable increase in the broadening of the peaks in the range of 0.8–1.4 ppm (Figs. 8C and S8C, green mark). These peaks were attributed to the formation of small aggregates composed of DMPC and TX-100. The broad peaks assignable to the DMPC lipids were similar to those observed in LMI**10**, LMI**11** and LMI**16**. However, DLS measurements revealed that the D_{hy} value of the liposomes decreased slightly from 88 to 74 nm following the addition of TX-100 (30 mol%) (Table 2), which was similar to the changes observed for guest molecules **10**, **11** and **16** in category (iii). In contrast, much sharper peaks were observed for both TX-100 and DMPC in the range of 0.8–1.4 ppm after the TX-100-mediated collapse of all of the liposomes ([TX-100]/[DMPC] =

1000 mol%) (Figs. 8D and S8D). Furthermore, after all of the DMPC liposomes had collapsed based on their peak intensities, the D_{hy} value was determined to be 8 nm by DLS (Table 2), which clearly indicated that all the DMPC molecules had formed very small micelles with TX-100. The broadening of the peaks in Fig. 8C indicated that the small aggregates formed between DMPC and TX-100 at 30 mol% were larger than the micelles formed by TX-100. The results observed for TX-100 strongly support the formation of small aggregates in LMI**10**, LMI**11** and LMI**16** (Scheme 1C). The small aggregates formed by the addition of **10** were also not complete small micelles but rather large micelles or small liposomes. In fact, for [**10**]/[DMPC] = 30 mol%, the peaks in the range of 0.8–1.4 ppm became sharper than those observed at 10 mol%. Unfortunately, it was not possible to investigate the effects of adding more **10** because it was not all incorporated in the lipid membranes for [**10**]/[DMPC] > 50 mol% by UV-vis absorption analysis.

3.4.2 Inhibiting the formation of small aggregates. We considered that the formation of small aggregates could be attributed to the lability of the DMPC liposomes. These spectra were measured at 25 °C, which is above the phase transition temperature (T_m) between the gel and liquid-crystal phases of the DMPC liposomes (T_m = 23 °C). To determine the effect in the gel phase with the tight packing of the hydrophobic chains, we carried out ^{1}H NMR measurement involving LMI**10** at a temperature below the T_m of LMI**10**. As shown in Figs. 5C, 9A 9B, S9A and S9B, the ^{1}H NMR spectrum of an LMI**10** solution recorded at 20 °C showed that the peaks observed in the range of 0.8–1.4 ppm were not as broad as those observed at temperatures of 25 and 30 °C (>T_m). The result indicated that while the gel phase of the DMPC liposomes could prevent the formation of small aggregates, it could not do so completely. Based on this result we prepared LMI**10** consisting of DPPC, which has been reported to form much more stable liposomes than DMPC. Figs. 9C–9E and S9C–S9E show the ^{1}H NMR spectra of LMI**10** consisting of DPPC liposomes at 25, 37 (body temperature) and 50 °C, respectively. The intensities of the broadened peaks in the range of 0.8–1.4 ppm increased with increasing temperature, indicating that the temperature has a

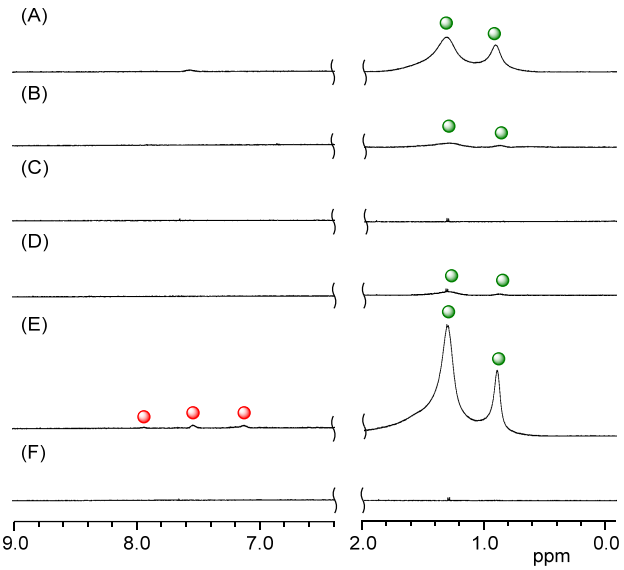

Fig. 9 Partial ^{1}H NMR spectra of LMI**10** consisting of DMPC in D_2O at (A) 30 °C and (B) 20 °C and LMI**10** consisting of DPPC in D_2O at (C) 25 °C, (D) 37 °C and (E) 50 °C followed by cooling to (F) 25 °C (●: guest molecule and ●: DMPC lipids in the small aggregates). [**10**]/[lipid] = 10.0 mol%, [lipid] = 4.0 mM, [DMSO] = 0.4 mM.

much greater influence on the formation of the small aggregates than T_m. After cooling at 25 °C (Figs. 9F and S9F), the spectrum returned to what it was before heating (Fig. 9C), indicating that the formation of the small self-aggregates was a reversible process. In contrast, LMI**11** and LMI**16** gave new broadened peaks in the range of 7.0–9.0 ppm (Figs. 10D, 10E, S10D and S10E). These results indicated that the more stable DPPC liposomes had prevented the formation of small aggregates to a much greater extent than the DMPC liposomes, whereas **11** and **16** were released from the DPPC liposomes and consequently included in category (iv). Furthermore, the peaks observed in the ^{1}H NMR spectra of LMI**5**, **6** and LMI**17**–**19** in the ranges of 7.0–9.0 ppm did not disappear after cooling at 25 °C (Figs. 10B, 10C, 10F–H, S10B, S10C and S10F–H), indicating that **5**, **6** and **17**–**19** remained in category (iv) even by use of DPPC liposomes. In contrast, the broadened peaks observed in the ^{1}H NMR spectra of LMI**4** in the ranges of 0.8–1.4 and 7.0–9.0 ppm disappeared after cooling at 25 °C (Figs. 10A and S10A), indicating that most of the guest molecules formed stable LMIGs in the same manner as those in category (i).

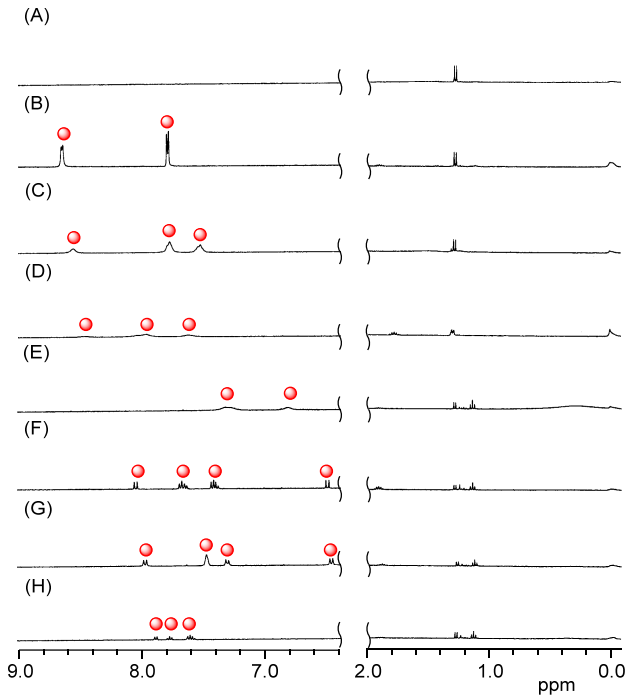

Fig. 10 Partial ^{1}H NMR spectra of (A) LMI**4**, (B) LMI**5**, (C) LMI**6**, (D) LMI**11**, (E) LMI**16**, (F) LMI**17** (G) LMI**18** and (H) LMI**19** consisting of DPPC in D_2O at 25 °C (●: guest molecule). [**4**, **5**, **6**, **11**, **16**, **17**, **18** or **19**]/[DPPC] = 10.0 mol%, [DPPC] = 4.0 mM, [DMSO] = 0.4 mM.

3.4.3 Relationship between the abundance of the compound in the lipid membrane and its log *P*ow value. The log P_{ow} value of a guest molecule is usually defined as the ratio of its concentrations in the two phases of a biphasic mixture composed of 1-octanol and water. Although the log P_{ow} values of guest molecules are usually determined experimentally, it is also possible to estimate these value using several commercially available computer programs.[31]

For log P_{ow} > 1.9, most of the compounds belonged to category (i) (Fig. 11, black) and formed stable LMIGs. Although compound **4** (log P_{ow} > 2.59) was category (iv) (Fig. 11, red), the leakage percentage of **4** was 5%. For log P_{ow} < 1.9, most of the compounds belonged to category (iv) (Fig. 11, red) except for compound **16**. Thus, although this value cannot be used to explain the behaviors of all of the guest compounds, the threshold for the leakage of the guest molecules was determined to be approximately 1.9. The threshold toward the DMPC and DPPC liposomes is almost same (Fig. 11, open red squares and triangle).

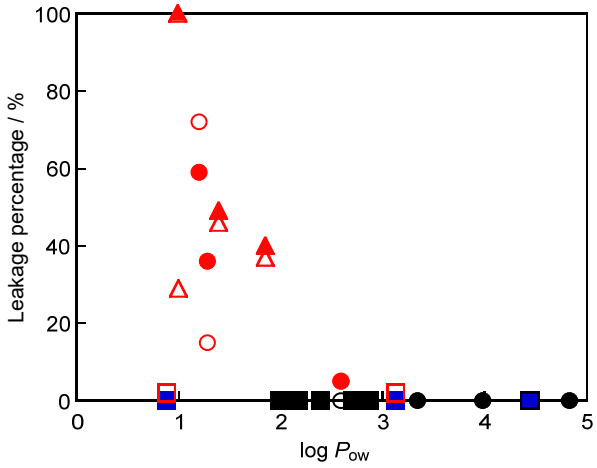

Fig. 11 Comparison of the leakage percentages of the guest molecules with the log P_{ow} values of compounds **1**–**6** (circle), **8**–**16** (square) and **17**–**19** (triangle); DMPC (closed) and DPPC (open) liposomes; categories (i) (black), (iii) (blue) and (iv) (red), in D_2O at 25 °C. [G]/[lipid] = 10.0 mol%, [lipid] = 4.0 mM, [DMSO] = 0.4 mM.

4. Conclusions

LMIGs can be classified into four different categories, including (i) systems where most of the guest molecules have been incorporated into liposomes to form stable LMIGs; (ii) systems were some of the guest molecules precipitate from solution; (iii) systems were some of the guest molecules form small self-aggregates with lipids; and (iv) systems were some of the guest molecules leak from the lipid membranes and dissolve in the bulk water. Compounds **7** and **12** were included in category (ii) together with the fullerenes and porphyrins in the LMIGs that were prepared by the premixing method. In the premixing method, thin membranes are formed following the concentration of an organic solution of the lipids and guest molecules. The guest molecules included in category (ii) therefore formed larger self-aggregates of the guest molecules than any of the other guest molecules because of their poor solubility in organic solvents. Compounds belonging to categories (i), (iii) and (iv) could be distinguished based on their ^{1}H NMR spectra because all of the peaks belonging to the guest molecules and the lipids disappeared completely in their LMIGs. Compounds **1**–**3**, **8**, **9** and **13**–**15** were included in category (i) in the DMPC liposomes and formed stable LMIGs. All of these compounds had relatively high log P_{ow} values (> 1.9). Although compound **4** had similarly high log P_{ow} value (2.59), it showed some leakage (leakage percentage = 5%). In contrast, it was difficult to categorize compounds **10**, **11** and **16**, which were ultimately included in category (iii). These behaviors of these systems appeared to be influenced by a local increase in the curvature as a geometric consequence of the incorporation of cone-like guest molecules into the phospholipid bilayers. Compounds **5**, **6** and **17**–**19** were all included in category (iv) with relatively low log P_{ow} values (< 1.9). The border between categories (i) and (iv) was defined by log P_{ow} values in the range of 1.9–2.0 towards DMPC and DPPC liposomes. Further work towards better defining these categories is currently underway

in our laboratories using several other guest molecules and lipids.

Acknowledgements

This work was supported by the Japanese Society for the Promotion of Science (JSPS) KAKENHI Grant-in-Aid for Scientific Research (B) (Grant No. JP16H04133) and a Grant-in-Aid for Challenging Exploratory Research (Grant No. JP16K13982). The authors would like to express their deepest gratitude to Ms S. Fujita, Graduate School of Materials Science, Nara Institute of Science and Technology for providing technical assistance with the cryo-TEM observations.

Notes and references

1 A. D. Bangham, *Prog. Biophys. Mol. Biol*., 1968, **18**, 29–36.
2 G. Sessa and G. Weissmann, *J. Lipid Res.*, 1968, **9**, 310–318.
3 Y. Kaneda, *Adv. Drug Delivery Rev.*, 2000, **43**, 197–205.
4 T. M. Allen and P. R. Cullis, *Science*, 2004, **303**, 1818–1822.
5 V. P. Torchilin, *Nat. Rev. Drug Discovery*, 2005, **4**, 145–160.
6 H. I. Pass, *J. Natl. Cancer Inst.*, 1993, **85**, 443–456.
7 T. J. Dougherty, C. Gomer, B. W. Henderson, G. Jori, D. Kessel, M. Korbelik, J. Moan and Q. Peng, *J. Natl. Cancer Inst*., 1998, **90**, 889–905.
8 K. Lang, J. Mosinger and D. M. Wagnerová, *Coord. Chem. Rev*., 2004, **248**, 321–350 and references therein.
9 P. L. Felgner, T. R. Gadek, M. Holm, R. Roman, H. W. Chan, M. Wenz, J. P. Northrop, G. M. Ringold and M. Danielsen, *Proc. Natl. Acad. Sci. U. S. A*., 1987, **84**, 7413–7417.
10 *Liposomes: A Practical Approach*, ed. V. P. Torchilin and W. Weissig, Oxford University Press, Oxford, 2nd edn, 2003.
11 A. Ikeda, S. Hino, T. Mae, Y. Tsuchiya, K. Sugikawa, M. Tsukamoto, K. Yasuhara, H. Shigeto, H. Funabashi, A. Kuroda and M. Akiyama, *RSC Adv.*, 2015, **5**, 105279–105287.
12 A. Ikeda, *Chem. Rec*., 2016, **16**, 249–260.
13 A. Ikeda, T. Sato, K. Kitamura, K. Nishiguchi, Y. Sasaki, J. Kikuchi, T. Ogawa, K. Yogo and T. Takeya, *Org. Biomol. Chem*., **2005**, *3*, 2907–2909.
14 A. Ikeda, Y. Doi, K. Nishiguchi, K. Kitamura, M. Hashizume, J. Kikuchi, K. Yogo, T. Ogawa and T. Takeya, *Org. Biomol. Chem*., 2007, **5**, 1158–1160.
15 A. Ikeda, Y. Doi, M. Hashizume, J. Kikuchi and T. Konishi, *J. Am. Chem. Soc.,* 2007, **129**, 4140–4141.
16 Y. Doi, A. Ikeda, M. Akiyama, M. Nagano, T. Shigematsu, T. Ogawa, T. Takeya and T. Nagasaki, *Chem.-Eur. J.,* 2008, **14**, 8892–8897.
17 A. Ikeda, T. Sue, M. Akiyama, K. Fujioka, T. Shigematsu, Y. Doi, J. Kikuchi, T. Konishi and R. Nakajima, *Org. Lett.,* 2008, **10**, 4077–4080.
18 A. Ikeda, M. Nagano, M. Akiyama, M. Matsumoto, S. Ito, M. Mukai, M. Hashizume, J. Kikuchi, K. Katagiri, T. Ogawa and T. Takeya, *Chem.–Asian J*., 2009, **4**, 199–205.
19 A. Ikeda, Y. Kawai, J. Kikuchi and M. Akiyama, *Chem. Commun.,* 2010, **46**, 2847–2849.
20 A. Ikeda, M. Akiyama, T. Ogawa and T. Takeya, *ACS Med. Chem. Lett*., 2010, **1**, 115–119.
21 A. Ikeda, Y. Kawai, J. Kikuchi, M. Akiyama, E. Nakata, Y. Uto and H. Hori, *Org. Biomol. Chem*., 2011, **9**, 2622–2627.
22 A. Ikeda, K. Kiguchi, T. Shigematsu, K. Nobusawa, J. Kikuchi and M. Akiyama, *Chem. Commun.,* 2011, **47**, 12095–12097.
23 A. Ikeda, T. Hida, T. Iizuka, M. Tsukamoto, J. Kikuchi and K. Yasuhara, *Chem. Commun*., 2014, **50**, 1288–1291.
24 A. Ikeda, S. Hino, T. Mae, Y. Tsuchiya, K. Sugikawa, M. Tsukamoto, K. Yasuhara, H. Shigeto, H. Funabashi, A. Kuroda and M. Akiyama, *RSC Adv.*, 2015, **5**, 105279–105287.
25 A. Ikeda, M. Mori, K. Kiguchi, K. Yasuhara, J. Kikuchi, K. Nobusawa, M. Akiyama, M. Hashizume, T. Ogawa and T. Takeya, *Chem.–Asian J*., 2012, **7**, 605–613.
26 A. Ikeda, *Chem. Rec*., 2016, **16**, 249–260.
27 Y. Katz and J. M. Diamond, *J. Membrane Biol.*, 1974, **17**, 69–86.
28 S. T. Burns and M.G. Khaledi, *J. Pharm. Sci*., 2002, **91**, 1601–1612.
29 A. Klamt U. Huniar, S. Spycher and J. Keldenich, *J. Phys. Chem. B*, 2008, **112**, 12148−12157.
30 S. Endo, B. I. Escher and K.-U. Goss, *Environ. Sci. Technol.*, 2011, **45**, 5912–5921.
31 The values of log P_{ow} were calculated using Advaced Chemistry Development Software V11.02 (ACD/labs.).
32 A. Ikeda, T. Hida, T. Nakano, S. Hino, K. Nobusawa, M. Akiyama and K. Sugikawa, *Chem. Lett*., 2014, **43**, 1551–1553.
33 K. Nakazawa, M. Hishida, S. Nagatomo, Y. Yamamura and K. Saito, *Chem. Lett.*, 2014, **43**, 1352–1354.
34 A. Ikeda, S. Hino, K. Ashizawa, K. Sugikawa, J. Kikuchi, M. Tsukamoto and K. Yasuhara, *Org. Biomol. Chem.*, 2015, **13**, 6175−6182.
35 J. Lasch, *Biochim. Biophys. Acta*, 1995, **1241**, 269–292.
36 H. Heerklotz, *Quart. Rev. Biophys*., 2008, **41**, 205–264.
37 M. A. Perillo and D. A. Garcia, *Colloids Surf., B*, 2001, **20**, 63−72.
38 Y. Cohen, H. Weitman, M. Afri, R. Yanus, S. Rudnick, Y. Talmon, J. Schmidt, P. Aped, S. Shatz, B., Ehrenberg and A. A. Frimer, *J. Liposome Res*., 2012, **22**, 306–318.
39 S. M. K. Davidson and S. L. Regen, *Chem. Rev.*, 1997, **97**, 1269–1279 and references therein.
40 A. Mueller and D. F. O'Brien, *Chem. Rev.*, 2002, **102**, 727–757 and references therein.